AD-A109 332 NORMAL MODES ANALYSIS OF GUN VIBRATIONS BY THE UNIFORM SEGMENT METHOD(U) ARMY ARMAMENT RESEARCH DEVELOPMENT AND ENGINEERING CENTER WAT.. R G GAS NOV 87 1/1

UNCLASSIFIED ARCCB-TR-87033 F/G 19/6 NL

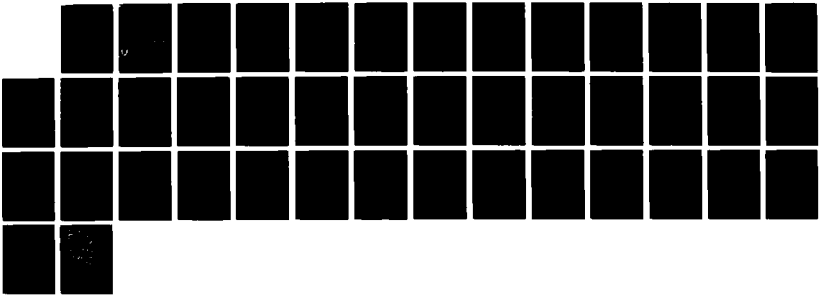

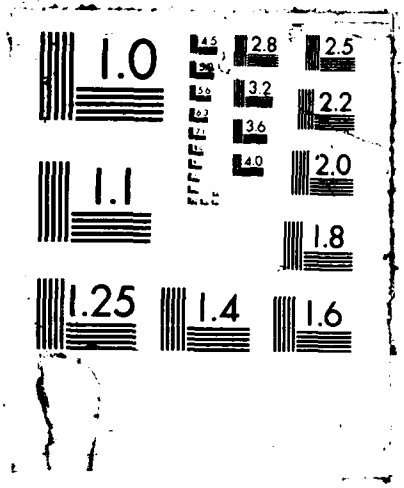
1.0
2.8
2.5
3.2
2.2
3.6
4.0
2.0
1.1
1.8
1.25
1.4
1.6

(4)

AD

TECHNICAL REPORT ARCCB-TR-87033

NORMAL MODES ANALYSIS OF GUN VIBRATIONS BY THE UNIFORM SEGMENT METHOD

RONALD G. GAST

NOVEMBER 1987

US ARMY ARMAMENT RESEARCH, DEVELOPMENT AND ENGINEERING CENTER
CLOSE COMBAT ARMAMENTS CENTER
BENÉT WEAPONS LABORATORY
WATERVLIET, N.Y. 12189-4050

DISCLAIMER

The findings in this report are not to be construed as an official Department of the Army position unless so designated by other authorized documents.

The use of trade name(s) and/or manufacturer(s) does not constitute an official indorsement or approval.

DESTRUCTION NOTICE

For classified documents, follow the procedures in DoD 5200.22-M, Industrial Security Manual, Section II-19 or DoD 5200.1-R, Information Security Program Regulation, Chapter IX.

For unclassified, limited documents, destroy by any method that will prevent disclosure of contents or reconstruction of the document.

For unclassified, unlimited documents, destroy when the report is no longer needed. Do not return it to the originator.

SECURITY CLASSIFICATION OF THIS PAGE (When Data Entered)

REPORT DOCUMENTATION PAGE		READ INSTRUCTIONS BEFORE COMPLETING FORM
1. REPORT NUMBER ARCCB-TR-87033	2. GOVT ACCESSION NO. AD-A189 332	3. RECIPIENT'S CATALOG NUMBER
4. TITLE (and Subtitle) NORMAL MODES ANALYSIS OF GUN VIBRATIONS BY THE UNIFORM SEGMENT METHOD		5. TYPE OF REPORT & PERIOD COVERED Final 6. PERFORMING ORG. REPORT NUMBER
7. AUTHOR(s) Ronald G. Gast		8. CONTRACT OR GRANT NUMBER(s)
9. PERFORMING ORGANIZATION NAME AND ADDRESS US Army ARDEC Benet Laboratories, SMCAR-CCB-TL Watervliet, NY 12189-4050		10. PROGRAM ELEMENT, PROJECT, TASK AREA & WORK UNIT NUMBERS AMCMS No. 6126.23.1BL0.011 PRON No. A1720518A11A
11. CONTROLLING OFFICE NAME AND ADDRESS US Army ARDEC Close Combat Armaments Center Picatinny Arsenal, NJ 07806-5000		12. REPORT DATE November 1987 13. NUMBER OF PAGES 34
14. MONITORING AGENCY NAME & ADDRESS(if different from Controlling Office)		15. SECURITY CLASS. (of this report) UNCLASSIFIED 15a. DECLASSIFICATION/DOWNGRADING SCHEDULE

16. DISTRIBUTION STATEMENT (of this Report)

Approved for public release; distribution unlimited.

17. DISTRIBUTION STATEMENT (of the abstract entered in Block 20, if different from Report)

18. SUPPLEMENTARY NOTES

Presented at the Fifth U.S. Army Symposium on Gun Dynamics, The Institute on Man and Science, Rensselaerville, New York, 23-25 September 1987. Published in Proceedings of the Symposium.

19. KEY WORDS (Continue on reverse side if necessary and identify by block number)

Vibrations	Elastic Supports
Modal Analysis	Numerical Methods
Beams	Gun Dynamics
Nonuniform Beams	Structural Dynamics

20. ABSTRACT (Continue on reverse side if necessary and identify by block number)

In a related paper published in the Proceedings of the Fourth US Army Symposium on Gun Dynamics (Sneck and Gast, "Normal Modes Analysis of Gun Dynamics"), the Euler-Bernoulli equation for a prismatic gun/beam elastically supported (transverse and rotation) at the breech was solved for its normal vibration modes and response to various transient loadings. This report is an extension of the reference in that the axially varying tube properties are now considered, whereas the boundary conditions are removed and applied as external displacement

(CONT'D ON REVERSE)

DD FORM 1 JAN 73 1473 EDITION OF 1 NOV 65 IS OBSOLETE

UNCLASSIFIED

SECURITY CLASSIFICATION OF THIS PAGE (When Data Entered)

20. ABSTRACT (CONT'D)

dependent loads.

In the Uniform Segment Method the spatial domain is divided into a finite number of prismatic sections within which the Euler equation is applied. Solutions to this equation yield functional relationships for mode shapes in the form of trigonometric and hyperbolic functions. The overall structure is modelled as a free-free beam with intersegment continuity assured by the matching of displacement, slope, moment, and shear transfer at segment boundaries. Applying the free-free boundary and continuity conditions results in a system of equations in the unknown frequencies and coefficients. The solution of this system yields the natural frequencies and mode shape coefficients within an arbitrary constant.

The main advantage of using this method over finite elements lies in the reduced number of degrees of freedom needed to model the structure. Real prismatic sections model one to one. This is not the case in finite element methods. Additionally, a number of the transient loads known to drive gun vibrations are functions of the mode shape derivatives. Since these functions are represented analytically, which is a characteristic of the Uniform Segment Method, the need to calculate derivatives by numerical algorithms is eliminated. Thus, exactness in derivative calculations is assured.

TABLE OF CONTENTS

LIST OF ILLUSTRATIONS

BACKGROUND

At the Fourth U.S. Army Symposium on Gun Dynamics, which convened in May 1985, the author, in collaboration with H. J. Sneck, submitted a paper (ref 1) in which a method for modelling the flexural vibrations of a tank gun using the normal modes technique was proposed and developed. In this report, a number of shortcomings in both the model and analysis techniques are cited and will be reviewed briefly.

The first and most striking model shortcoming lies in the use of an axially prismatic beam as representative of the gun tube knowing full well that a gun possessing a prismatic barrel does not exist. The reason for the choice, however, lies in the fact that although guns are axially non-uniform, their deviation from the prismatic condition is small when compared to their overall length. For example, when viewed from a distance, any gun appears to be of uniform cross section. A less important reason for this choice was the ease in which this type of model could be developed. For the prismatic case, a single four-term mode shape equation results for each natural frequency considered.

The second involves the choice of support conditions. In this initial effort, the supports were modelled as linear, bi-directional springs rigidly attached to the breech end (origin of axial coordinate) of the beam. One spring resisted the transverse displacement, while the second restrained the rotational motion of the breech end. This type of support model is not exact, but rather an approximation of what actually exists on fielded weapons. In addition, supports possessing no clearance are not feasible from an assembly or operational standpoint and those possessing linear response properties regarding force/deflection are not likely.

References are listed at the end of this report.

The third model shortcoming involves the use of the Euler-Bernoulli beam equation without a strong claim regarding its applicability for gun/beam type structures. It was chosen based upon the results of an order of magnitude study on the equation's coefficients for the model of a gun system similar to the M60. A more viable approach comparing the results of a modelling effort using alternative equations would be a better means of justification.

A fourth condition involves the identified excitation sources (driving loads) developed into the model. There were five sources which included recoil inertia, pressure curvature, projectile trajectory, projectile rotational imbalance, and eccentricity. These, by far, are the most important loading sources, however, a more versatile model employing additional sources would be more realistic.

All of the above areas are addressed in the current analysis. This report highlights the detailed improvements which have been developed into the current computer model dedicated to gun vibration analysis. The routines are available and running on Benet Laboratories VM/SP Operating System.

FORMULATION OF THE CANNON BEAM DYNAMICS MODEL

General Modelling Equation and Solution Proposal

Beam dynamics as applied to gun tubes is represented in Figure 1 where the beam structure shown possesses axially varying geometric properties inferring that both bending and inertial resistance are functions of position. The transverse cross section is cylindrical and axisymmetric, and in its static state, the axis assumes in-plane curvature due to the beam's weight, environmental condition, and the result of manufacturing processes. The features drawn in

phantom represent the additional mass of the breech, bore evacuator, and muzzle brake. Four types of forces and/or moments are represented and appropriately placed upon the structure.

CANNON/BEAM LOADING SCHEMATIC

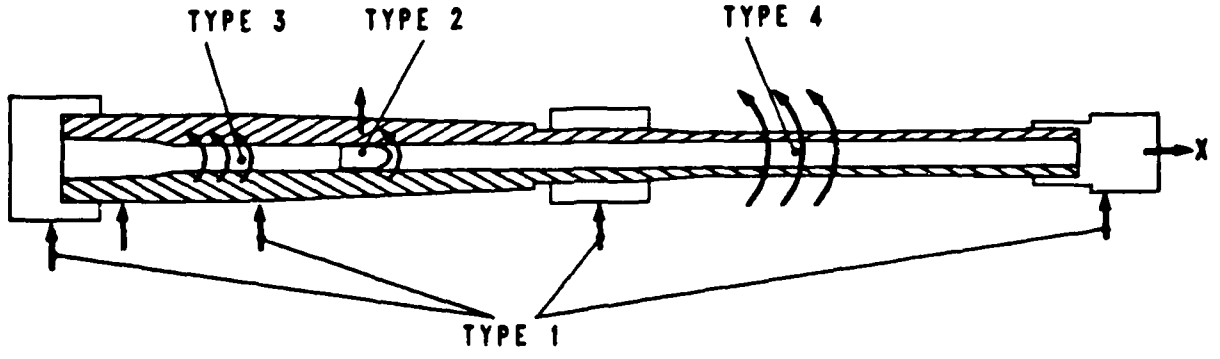

Figure 1. Cannon/beam loading schematic.

The equation which completely describes the transverse motion of this beam system according to Thomson (ref 2) and others (refs 3-6), is:

$$(EIy'')'' + \frac{w}{g}\ddot{y} - (J + \frac{EIw}{gkAG})\ddot{y}'' + (\frac{Jw}{gkAg})\ddot{y}'' = \sum_{i=1}^{N} [p_i(x,t,y,y',y'',\dot{y}') + \frac{J}{kAG}\dot{p}_i(x,t,y,y',y'',\dot{y}') - \frac{EI}{kAg}p_i''(x,t,y,y',y'',\dot{y}')] - w \qquad (1)$$

where

E = Young's Modulus of material

I = transverse moment of inertia

J = pitch moment of inertia

G = modulus of elasticity in shear

A = area of beam's cross section

k = shape factor of cross section

w = weight per unit length of beam

p_i = i-th forcing function (total of N)

g = gravity acceleration

x = axial coordinate (independent space variable)

t = time (independent time variable)

y = transverse displacement (dependent space variable)

$\dot{}$ = time derivative

$'$ = space derivative

This equation is commonly referred to as the Timoshenko equation. For a prismatic beam, the second differential operation on the first term could be placed within the brackets since the bending resistance becomes constant. The second term deals with the translational inertia of a beam segment, while the remaining two terms model rotatory inertia and shear deformation effects. All terms are on a per length basis. The right side of the equation contains the representative driving and reaction loads.

Reduced forms of this equation are used when the geometry causes some of the coefficients to be relatively insignificant. Other special cases arise for the analysis of prismatic beams for which all geometric properties are constant in space rendering all dependent variable coefficients constant. This allows for a closed-form solution to the homogeneous equation as will be addressed later. For 'thin' structures, terms involving rotatory inertia become small, thus modifying the coefficient of the third term and completely eliminating the fourth term. For 'long' structures, bending dominates shear, thus both terms three and four may be eliminated without loss of modelling accuracy. In this

simpler form, the Timoshenko equation reduces to the Euler-Bernoulli equation, which upon the stipulation of constant cross-sectional properties, becomes

$$EIy'''' + \frac{w}{g}\ddot{y} = \sum_{i=1}^{N} [p_i(x,t,y,y',y'',\dot{y}')] - w \qquad (2)$$

The solution technique for the proposed model in its full or any of the truncated forms is the same. The homogeneous equation will be solved by the separation of variables technique yielding the normal modes of vibration of a free-free beam structure. The model equation will be reassembled using the mode shape vectors, and upon invocation of the appropriate orthogonality principle, a system of ordinary differential equations (O.D.E.'s) containing time varying amplitude coefficients will result. There will be one equation for each mode shape considered. Due to the nature of the loadings, this system of O.D.E.'s is coupled; therefore, numerical matrix procedures will be needed to arrive at the total solution.

Assessing the Significance of Shear and Rotatory Inertia

The Timoshenko equation represents the most complete form of beam analysis available. For certain types of beam structures, the combined effect of shear deflection and rotatory inertia contributes little to the results while their inclusion is costly in terms of solution complexity. Since this modelling effort is to be applied to a certain class of structures, namely large caliber cannon tubes, these effects may be judiciously neglected in favor of the less complex Euler-Bernoulli model. The reason for this will be developed in the following comparative analysis of a uniform 'thin' beam.

Consider the free vibrations of an unrestrained prismatic beam. The Timoshenko equation (1) becomes

$$EIy'''' + \frac{w}{g}\ddot{y} - (J + \frac{EIw}{gkAG})\ddot{y}'' + (\frac{Jw}{gkAG})\ddot{y} = 0 \qquad (3)$$

Following the method used by Bozich (ref 4) and identifying the parameters suggested by Kruzlewski (ref 7), this equation may be reformulated in a dimensionless form.

$$\frac{1}{K_B^2}\left(\frac{d^4y}{dz^4}\right) + (K_R^2+K_S^2)\frac{d^2y}{dz^2} - (1 - K_B^2K_R^2K_S^2)y = 0 \qquad (4)$$

where

$$K_B^2 = \omega^2L^4\frac{w}{gEI} \qquad (5a)$$

$$K_S^2 = \frac{1}{L^2}\frac{EI}{kAG} \qquad (5b)$$

$$K_R^2 = \frac{1}{L^2}\frac{Jg}{w} \qquad (5c)$$

with ω being a vibration frequency. These three coefficients represent the contributions of bending, shear, and rotatory inertia, respectively. Equation (4) represents the non-dimensional form of the Timoshenko model which reduces to the Euler-Bernoulli version by simply setting K_S and K_R to zero.

In terms of the non-dimensional coordinate z, the analytical solution to the equation is

$$y(x,t) = (C_1 \cos \alpha z + C_2 \sin \alpha z + C_3 \cosh \beta z + C_4 \sinh \beta z)\cos \omega t \qquad (6)$$

where

$$\alpha = K_B\sqrt{\frac{+ (K_R^2+K_S^2) + \sqrt{(K_R^2-K_S^2) + 4/K_B^2}}{2}} \qquad (7a)$$

$$\beta = K_B\sqrt{\frac{- (K_R^2+K_S^2) + \sqrt{(K_R^2-K_S^2) + 4/K_B^2}}{2}} \qquad (7b)$$

These equations are valid when the terms within the outer radical remain positive. By applying free-free boundary conditions and normalizing the mode shapes with respect to C_1, the following characteristic equation for the natural frequencies may be derived:

$$2(1-\cos\alpha\cosh\beta) + \left(\frac{\beta^2-\alpha^2}{\alpha\beta}\right)\sin\alpha\sinh\beta = 0 \tag{8}$$

This equation, which is essentially a function of ω, has an infinite number of roots. It may be solved to any desired accuracy for a finite number of them by standard root finding techniques. A set of computer routines for solving this uniform beam frequency equation was written for the assessment analysis. The effect of shear deflection and rotatory inertia may be included or neglected in order that an evaluation of their effects may be made. The equation coefficients evaluated for each frequency are

$$C_1 = 1 \tag{9a}$$

$$C_2 = \left(\frac{\beta}{\alpha}\right)\left(\frac{\cos\alpha - \cosh\beta}{\sinh\beta - (\beta/\alpha)\sin\alpha}\right) \tag{9b}$$

$$C_3 = \left(\frac{\alpha}{\beta}\right)^2 \tag{9c}$$

$$C_4 = \left(\frac{\alpha}{\beta}\right)^3 C_2 \tag{9d}$$

These coefficients and their respective natural frequencies are used to evaluate and plot mode shapes as a function of the dimensionless coordinate z. The results, as calculated by the Timoshenko and Euler-Bernoulli models for a given structure, may then be compared to determine whether the shear deflection and rotatory inertia effects are significant for the class of beams to be analyzed.

In order to assess the effect of shear and rotatory inertia on cannon vibrations, three uniform cross section pipe structures resembling contemporary tank cannons were analyzed using this technique. The results of this analysis are contained in Figure 2 where the percent error (with respect to the full Timoshenko equation) is plotted against mode number for the three structures analyzed. The results indicate that both of the simpler models predict frequency values which are higher than those which the Timoshenko equation would yield. The 'thicker' structures are less accurate when the Euler-Bernoulli equation is used, however, the inclusion of rotatory inertia in the Timoshenko equation contributes very little for any of the structures. At an outer diameter of 8 inches, a 7.5 percent error in frequency would occur in the sixth mode using the simplest formulation, while only 1.5 percent error would result using the complex equation without rotatory inertia.

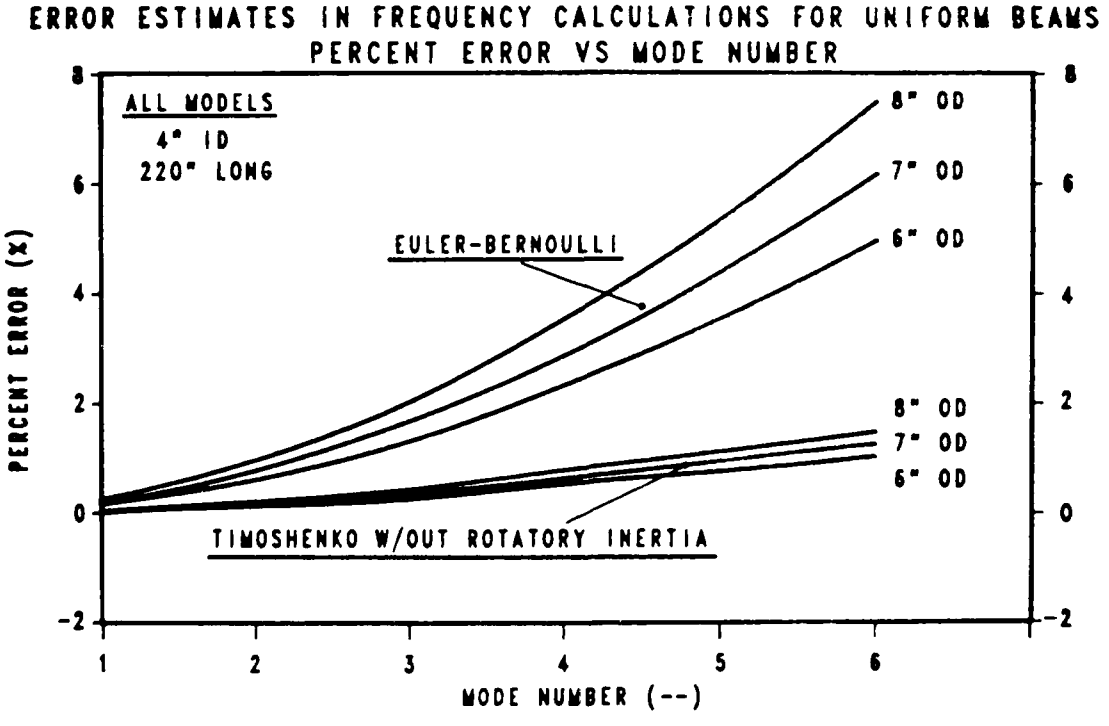

Figure 2. Error in frequency calculations for uniform beams.

A comparison of mode shapes for the sixth mode of the 8-inch beam is plotted in Figure 3. The upper curve represents the shape using the Timoshenko equation, while the lower is the same for the Euler-Bernoulli equation. As can be seen, they are quite similar except at the end points where a deflection error of -8.3 percent and a slope error of -0.75 percent results from the use of the simpler equation. Although this appears to be quite substantial, these error levels become less for the lower modes. Since mode shape contribution diminishes with increasing mode number, these error estimates become relatively unimportant to the overall transient response. In addition, a 220-inch long by 8-inch diameter 105-mm cannon is heftier than any fielded or developmental hardware, therefore, the reported errors become upper bounds when actual cannons are modelled. For these reasons, the Euler-Bernoulli formulation of the vibration equation was selected for the remainder of this analysis.

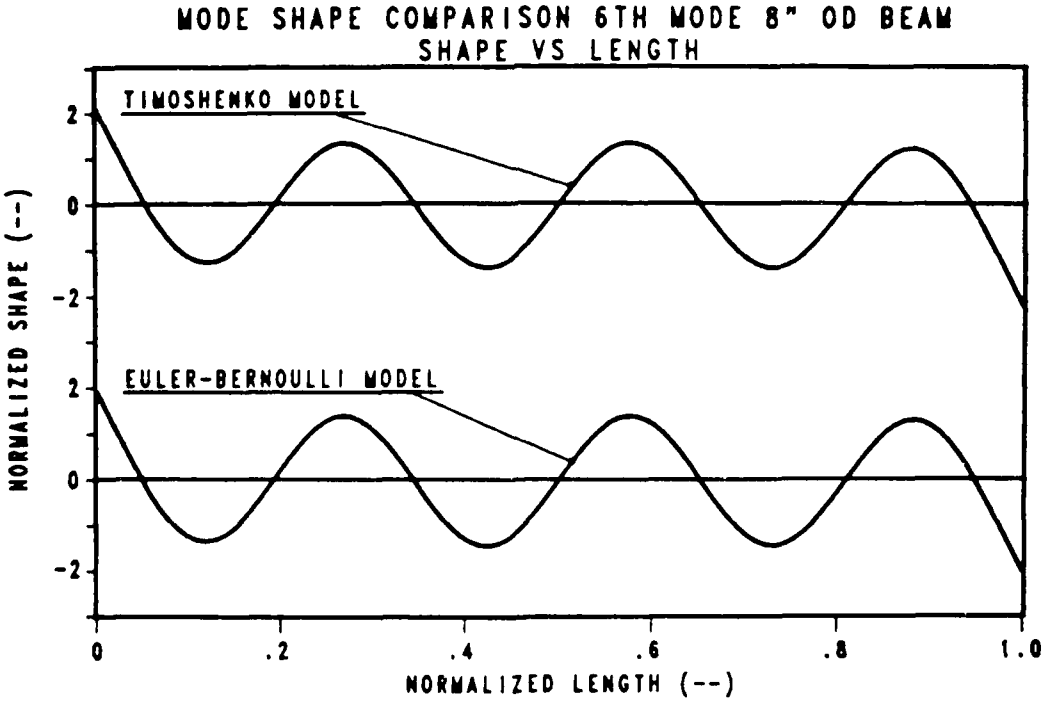

Figure 3. Mode shape comparison for uniform beam models.

Modelling the Non-Prismatic Effect

It goes without saying that the inclusion of non-prismatic geometries increases the complexity of this problem. The normal vibration functions for the uniform beam were shown to be analytic for any of the model equations chosen. This is a great advantage in solving transient problems where the modal functions need to be differentiated for certain types of driving loads. (This is especially true for gun tube loads as will be shown later.) If the modal function is approximated by a set of tabular values (e.g., numeric tables from finite element analysis), accurate differentiation is difficult, even when the points are connected by approximating polynomials. Since the non-uniform nature of a gun tube is consistent in that it is composed of cylindrical sections, tapered sections, and step changes between sections, attempting to solve the free vibration equation with a single analytical function may be impossible.

A number of approaches were found during the research phase of the study (refs 9-16). Each of these authors attempted to resolve the problem of modelling the flexural dynamics of a non-prismatic beam. All, however, fell short of expectations in terms of fulfilling the need for analytically expressible mode shape functions differentiable through the second order. Canned finite element routines were ruled out early due to the lack of versatility in their ability to model loads which are functions of the dependent variable. In regard to their employment for determining the mode shapes, the only way a continuous analytical function could be achieved was through a least squares or spline fit using the normal modes displacement information. This was unattractive since it is well known that modal displacements approach sinusoidal shapes for beams with mild non-uniformities. Any method developed for structures of this type should attempt to exploit this property.

Upon conversing with and reviewing the work of Dr. Sneck (ref 17), a method of dealing with the problem's non-prismatic nature was conceived. He suggested that the tube be divided into two uniform segments of differing cross sections, each of which is analyzed using the Euler-Bernoulli equation. By the separation of variables technique (refs 2,3), the application of the appropriate boundary conditions, and the enforcement of interfacial continuity at segment boundaries, expressions involving trigonometric and hyperbolic terms for the mode shape functions will result. Each segment will have its own set of mode dependent coefficients. Continuity across segment boundaries will be accomplished by equating boundary values of displacement, slope, bending moment, and shear as calculated by each adjacent mode function. This method seemed ideal for the problem at hand, and it was chosen contingent upon its adaptability to cannon models where more than two segments would be needed. It was felt that any number of segments could be handled by this method, hence, the term "Uniform Segment Method" (USM) was coined.

The equation defining the mode shapes for a general case employing the USM is

$$\phi_{ij}(\bar{x}) = A_{ij} \cosh \alpha_{ij}\bar{x} + B_{ij} \sinh \alpha_{ij}\bar{x} + C_{ij} \cos \alpha_{ij}\bar{x} + D_{ij} \sin \alpha_{ij}\bar{x} \qquad (10)$$

where:

i = segment number

j = mode shape number

$\bar{x}$ = normalized length (x/L)

A,B,C,D = mode shape coefficients

α_{ij} = argument coefficient $[L\sqrt{\omega_j}(\frac{1}{g}\ (\frac{w}{EI})_i)^{\frac{1}{4}}]$

By employing this segmented mode shape function and the well-known separation of variables technique on the pure bending equation, the unknown coefficients and

frequency for each mode may be tracked. For a model utilizing M sections, the imposition of the free-free boundary conditions will yield the following equations relating bending moment and shear at the extremities of the beam:

$$\phi''_{1,j}(0) = 0 \tag{11a}$$

$$\phi''_{M,j}(1) = 0 \tag{11b}$$

$$\phi'''_{1,j}(0) = 0 \tag{11c}$$

$$\phi'''_{M,j}(1) = 0 \tag{11d}$$

Continuity at the interfacial locations is preserved by equating the values of displacement, slope, bending moment, and shear as calculated by adjacent mode functions at the interfacial boundaries between segments. These conditions may be written as follows:

$$\phi_{i-1,j}(\bar{X}_{i-1}) = \phi_{i,j}(\bar{X}_{i-1}) \tag{12a}$$

$$\phi'_{i-1,j}(\bar{X}_{i-1}) = \phi'_{i,j}(\bar{X}_{i-1}) \tag{12b}$$

$$(EI)_{i-1}\phi''_{i-1,j}(\bar{X}_{i-1}) = (EI)_i\phi''_{i,j}(\bar{X}_{i-1}) \tag{12c}$$

$$(EI)_{i-1}\phi'''_{i-1,j}(\bar{X}_{i-1}) = (EI)_i\phi'''_{i,j}(\bar{X}_{i-1}) \tag{12d}$$

where:

i = segment number

$\bar{X}_k$ = normalized axial coordinate of segment k's right boundary

For a model containing M segments, there are 4M coefficients and one frequency to be evaluated for each mode shape. By setting $A_{1,j} = 1$ renders the system deterministic for which unique solutions exist at each natural frequency. A set of algebraic equations in the natural frequency (ω_j) and the 4M-1 unknown mode shape coefficients is presented in matrix form in Figure 4. The system matrix is shown to contain an orderly set of entries representing the boundary conditions (B.C.) and matching conditions (M.C.). A 2X4 subarray beginning at

global location 1,1 contains the terms for evaluating the B.C. at $\bar{x} = 0$, whereas a similar array ending at N,N (N=4M) represents the B.C. at $\bar{x} = 1$. 'Walking' along the main diagonal are M-1 subarrays 4X8 in size which represent the preservation of continuity across segment boundaries. The remaining terms in the matrix are zero. The non-zero entries are functions of the segment properties, boundary location, and the unknown natural vibration frequencies. Setting the determinant equal to zero and solving for the roots of the resulting characteristic equation produces values for these frequencies. At each frequency, a reduced system is developed by setting $A_{1,j} = 1$, eliminating the first row, and shifting the first column to the right side of the equation. The solution to this linear system yields the remaining normalized mode shape coefficients.

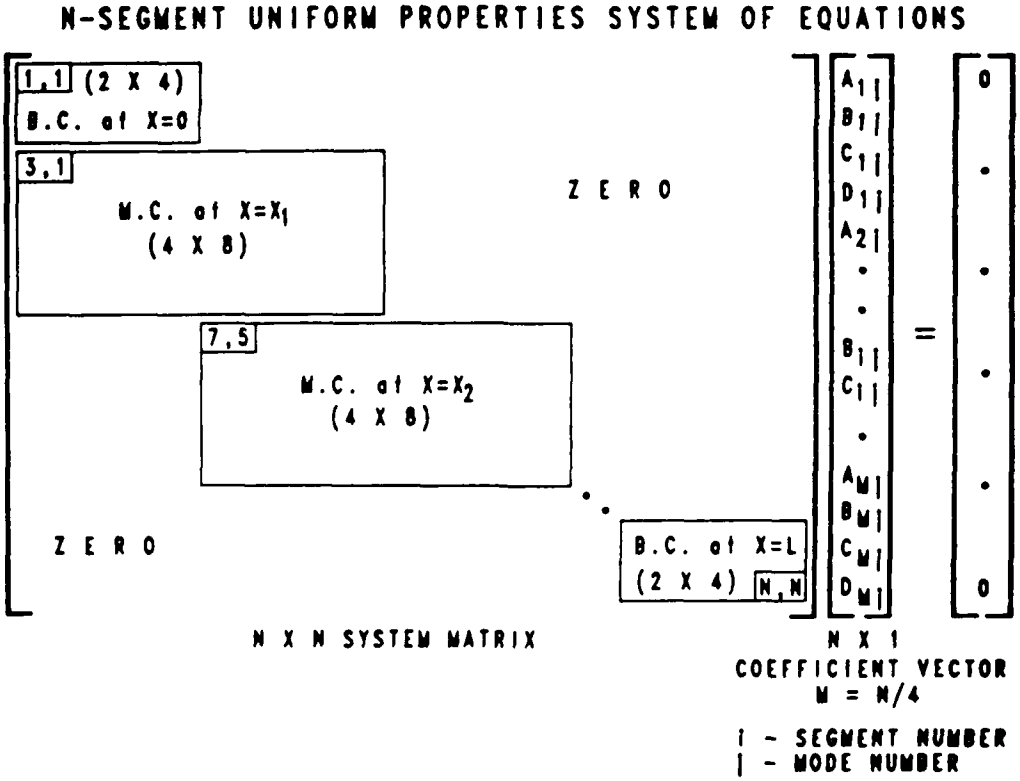

Figure 4. Uniform segment system of equations.

Unlike finite element techniques, this method does not require the segmenting of uniform sections. Rather, they transform on a one-to-one basis from the real to the model plane, thus only a few segments are needed to accurately represent gently varying non-uniformities. Additionally, the number of modes available for calculation is not a function of the number of segments. In finite elements, the mode shapes are defined by the displaced locations of the model's nodes. There are not enough points available for an accurate representation of the mode's shapes at higher natural frequencies. This is not the case for the USM, since nodeless elements using trigonometric and hyperbolic terms in the mode shape functions are employed.

To determine the accuracy of this method for free vibration modelling of gun structures, the predictions from an established finite element code (ABAQUS (ref 18)) for a typical gun tube (105-mm M68) were compared to the results generated by the dedicated routines (MODE:) written by the author in support of this analysis. The gun and its modelling representations are shown in Figure 5.

The M68 gun tube is 210 inches long containing two tapered and three cylindrical sections. The physical schematic is shown in the top sketch in Figure 5. This finite element model (FEM) was comprised of 54 equally-spaced nodes with two degrees of freedom (dof) per node and 53 prismatic beam elements. The sketch in the middle of the figure indicates the element density in each physical section of the structure. On the lower sketch of the same figure, segmentation of the USM model is shown. Only six segments of four dof each were used for a total of 24 dof. The natural frequencies and mode shapes for the first six vibration modes were calculated using both the Timoshenko and Euler equations for the FEM. In the USM analysis, only the Euler equation is employed.

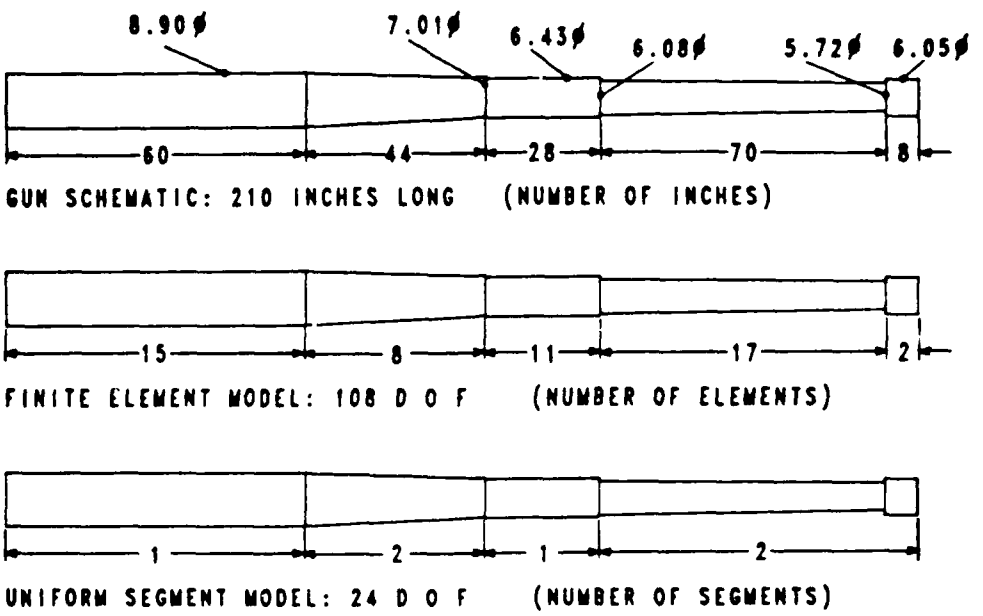

Figure 5. 105-mm M68 Gun: Comparison of analytical models.

The results of the analysis are shown in Figures 6 and 7. In Figure 6 a comparison among the frequency calculations is presented in the form of a bar graph. The abscissa contains the first six mode numbers, while the ordinate is labelled with the Log_{10} value of the frequency. As is indicated, the FEM using the Timoshenko equation produces the lowest values for all six frequencies, while the USM produces the highest. The differences in the extremes are between six and ten percent with the greatest discrepancy occurring at the highest mode number.

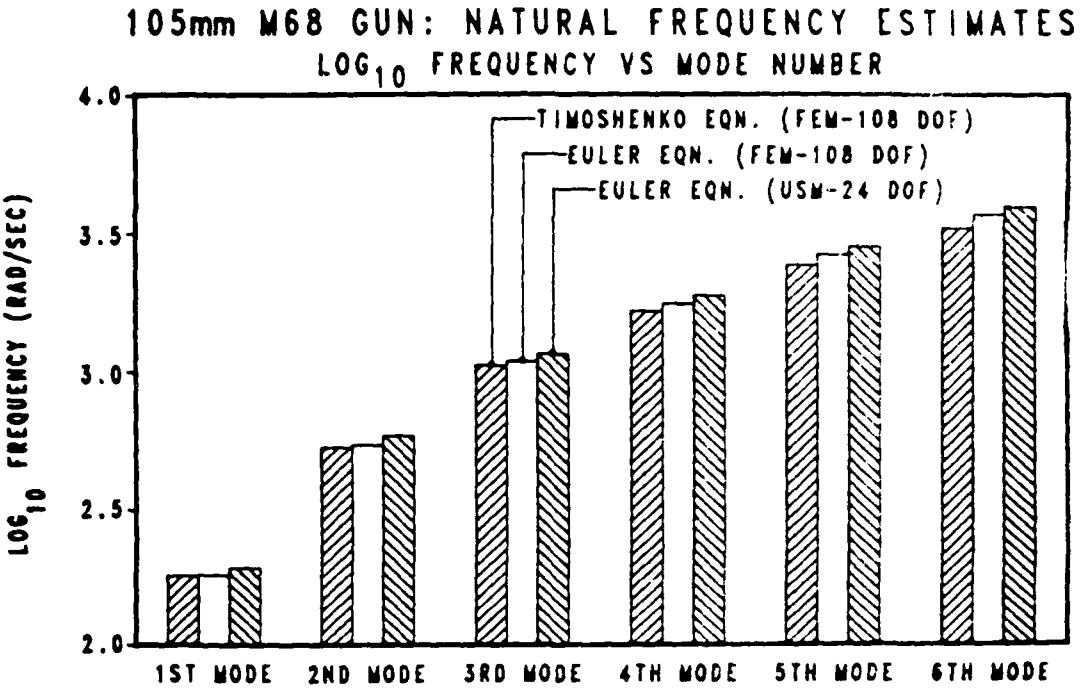

Figure 6. 105-mm M68 Gun: Natural frequency estimates.

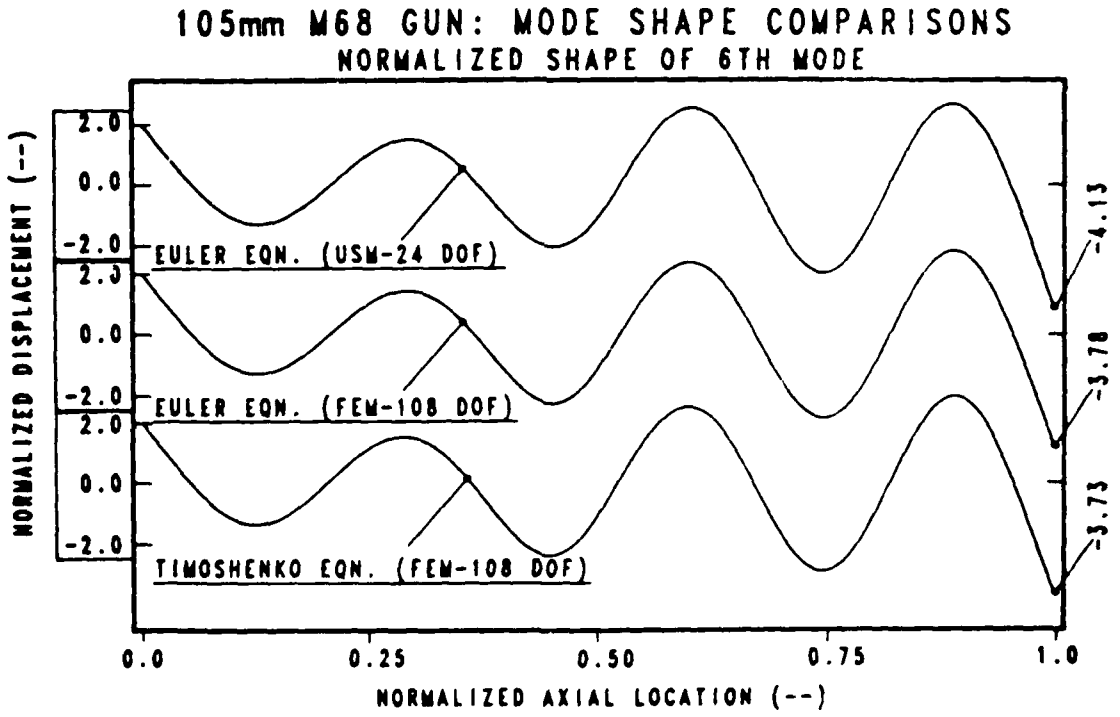

Figure 7. 105-mm M68 Gun: Mode shape comparison.

In Figure 7 the normalized mode shape plots for the sixth mode, as calculated by each of the models, is shown. The sinusoidal nature of the mode shape is evident on all three plots, while the subtle differences in displacement magnitude at the extreme end are perceptively indiscernible. Numerically, the magnitude of the displacement for the USM calculation is approximately ten percent higher than either of the other two FEM's. Overall, these results verify the worth of the USM in modelling mildly discontinuous beam structures. If greater accuracy is desired, more segments could be used for the tapered portions of the structure.

Modelling Initial Curvature

It is a generally accepted fact that the initial shape of the gun tube has a significant effect upon its dynamic response and shot accuracy. This dependence has been shown experimentally (Elder (ref 19)) as well as analytically (Simkins (ref 20), Warken (ref 21)). Four prominent causes of static gun/beam curvature, which are part of the proposed model, are

1. Gravity droop
2. Thermal droop
3. Manufacturing tolerances
4. Non-structural weight (breech, etc.)

To implement these effects, an independent set of routines (INIT:) was developed to generate the initial conditions for the gun/beam. These routines accept the geometry from the normal modes analysis, adding two resilient supports, point loads simulating non-structural mass, and distributed loads representing each segment's weight. The deflection response of the supports may include clearance and non-linear elasticity. Initially, the rigid body solution for the gun/beam is solved. This yields support reactions, deflections, and the

initial slope of the gun's axis. In the next portion, the static bending of the gun/beam due to weight and external mass is determined by numerical integration of the Euler-Bernoulli equation applied to the static case. The support reactions are redefined as external loads and their axial locations as points of zero bending deflection. This type of modelling is straightforward and well documented in structural mechanics literature (ref 22). Thermal response and manufacturing induced curvature are currently imported into this model via tabular files developed by empirical data or external analysis. The total vertical deflection is calculated by superimposing the individual responses and generating tabular files which will be used as data in the transient analysis.

Problem Closure: The Total Dynamic Response

Application of Orthogonality

Having a piecewise functional representation for the mode shapes and an approximating polynomial equation for initial deflection, closure to the problem involves solving particular forms of Eq. (2). Recalling:

$$EIy'''' + \frac{w}{g}\ddot{y} = \sum_{i=1}^{N} [p_i(x,t,y,y',y'',\dot{y}')] - w \qquad (2)$$

is the equation for a uniform beam. The dependent variable (y) contains both static and dynamic terms. By separating the dependent variable thusly, this equation may be recast and rewritten on a per segment basis as follows:

$$(EI)_k \left[\sum_{i=1}^{I} \phi_{ki} q_i + y_s \right]'''' + \frac{w_k}{g} \frac{\partial^2}{\partial t^2} \left[\sum_{i=1}^{I} \phi_{ki} q_i + y_s \right] =$$

$$\sum_{m=1}^{M} p_m(x,t,y,y',\dot{y},\ddot{y},y'',\dot{y}') - w_k(y) \qquad (13)$$

where:

i = i-th mode shape

I = total number of modes

k = k-th uniform segment

K = total number of segments

m = m-th applied load

M = total applied loads

$(EI)_k$ = bending resistance of k-th segment

w_k = weight/length of k-th segment

ϕ_{ki} = i-th mode shape of k-th segment

q_i = i-th modal amplitude

$p_m(x,t,...)$ = m-th applied load function

$W_k(y)$ = static mass load applied to k-th segment

y_s = static deflection curve

Since the modal amplitudes are time-dependent only and the static deflection is space-dependent only, the above equation may be separated as follows:

$$(EI)_k \left(\sum_{i=1}^{I} \phi_{ki} q_i'''' \right) + \frac{w_k}{g} \left(\sum_{i=1}^{I} \phi_{ki} \ddot{q}_i \right) = \sum_{m=1}^{M} p_m(x,t,...) \qquad (14a)$$

$$(EI)_k \, y_s'''' = W_k(y) \qquad (14b)$$

The solution to Eq. (14a) yields the dynamic response with respect to the initial shape of the beam. The solution to the second equation is the static deflection. Superposition of these leads to the total dynamic response with respect to a global inertial coordinate system. Since Eq. (14b) has already been solved (last section), the solution to Eq. (14a) will close the problem.

By the nature of the segment mode shape functions

$$\phi_{ki}'''' = \left(\frac{\alpha_{ki}}{L}\right)^4 \phi_{ki} \tag{15}$$

which leads to

$$\sum_{i=1}^{I} \phi_{ki}\left[\ddot{q}_i + g\left(\frac{EI}{w}\right)_k \left(\frac{\alpha_{ki}}{L}\right)^4 q_i\right] = \frac{g}{w_k}\left[\sum_{m=1}^{M} p_m(x,t,\ldots)\right] \tag{16}$$

Recalling a parameter from Eq. (10) and employing current notation

$$\alpha_{ki} = L\sqrt{\omega_i}\ \left(\frac{1}{g}\left[\frac{w}{EI}\right]_k\right)^{\frac{1}{4}}$$

which upon substitution yields

$$\sum_{i=1}^{I} \phi_{ki}[\ddot{q}_i + \omega_i^2 q_i] = \frac{g}{w_k}\left[\sum_{m=1}^{M} p_m(x,t,\ldots)\right] \tag{17}$$

For non-dissipative boundary conditions, the orthogonality of the mode shapes with respect to the weight function w(x)/g leads to the following:

$$\int_0^L \frac{w(x)}{g}\,\phi_i\phi_j\,dx = \sum_{k=1}^{K} \int_{x_{k0}}^{x_{k1}} \frac{w_k}{g}\,\phi_{ki}\phi_{kj}\,dx =$$

$$0 \quad \text{for } i \neq j \tag{18a}$$

$$G_i \quad \text{for } i = j \tag{18b}$$

where

x_{k0} = axial location of lower boundary of segment k

x_{k1} = axial location of upper boundary of segment k

Note: $x_{k1} = x_{(k+1)0}$

w(x) = structural weight distribution

By multiplying Eq. (17) by $\frac{w(x)}{g}\phi_i$, integrating over the length and applying Eq. (18), the following ordinary differential for modal amplitudes results:

$$\ddot{q}_i + \omega_i^2 q_i = \frac{1}{\bar{G}_i} \sum_{m=1}^{M} \sum_{k=1}^{K} \int_{x_{k0}}^{x_{k1}} p_m(x,t,\ldots)\phi_{ki}\, dx \tag{19}$$

The solution to this equation yields a vector of modal amplitudes used to calculate the dynamic displacement, velocities, and slopes. These equations are as follows:

$$y_d(x) = \sum_{i=1}^{I} q_i(t)\phi_i(x) \tag{20a}$$

$$\dot{y}_d(x) = \sum_{i=1}^{I} \dot{q}_i(t)\phi_i(x) \tag{20b}$$

$$y'(x) = \sum_{i=1}^{I} q_i(t)\phi_i'(x) \tag{20c}$$

where

$\phi_i(x) = \phi_{ki}(x_k)$ segment mode shape

Representation of the Forcing Functions

Previous analyses and test results indicate that static droop dominates the overall curvature. Dynamic response is shown to be a displacement perturbation about the static shape. The maximum displacement levels are an order of magnitude less than the static muzzle deflection. Since the loading functions unique to gun dynamics are dependent upon a gun's overall shape, so is the dynamic response. Recalling the functional form for these load functions

$$p_m(x,t,y,y',\dot{y},\ddot{y},y'',\dot{y}')$$

from Eq. (14a), the following expression from Eq. (19)

$$\frac{1}{G_i} \sum_{m=1}^{M} \sum_{k=1}^{K} \int_{x_{k0}}^{x_{k1}} p_m(x,t,\ldots)\phi_{ki}\, dx$$

must be evaluated for each load function considered. These load functions and evaluations will now be presented and discussed.

1. Recoil inertial load. An inertia couple develops within any segment k during recoil which is expressible as

$$p_1(t,x,y') = \frac{w_k}{g} a_r(t)[(\ell-x)y']' \tag{21}$$

where

$a_r(t)$ = recoil acceleration

ℓ = total length of gun

y = total transverse displacement (static and dynamic)

Details of the derivation may be found in Reference 20. Evaluation of the expression

$$\frac{1}{G_i} \int_o^{\ell} \frac{w_k}{g} a_r(t)[(\ell-x)y']'\phi_{ki}\, dx$$

upon the substitution of

$$y = \sum_{j=1}^{I} \phi_{kj}q_j + y_s \tag{22}$$

and normalizing with respect to tube length yields the following:

$$\frac{1}{G_i}\int_o^{\ell} p_1(x,t,y')\phi_{ki}\,dx = K_1(t)\{w_k\phi_{kj}[(1-\bar{x})(\sum_{j=1}^{I}\phi'_{kj}q_j+y'_s)]_{\bar{x}_{k0}}^{\bar{x}_{k1}}$$

$$-\ell\int_0^1 w_k\phi'_{ki}[(1-\bar{x})(\sum_{j=1}^{I}\phi'_{kj}q_j + y'_s)]d\bar{x}\} \qquad (23)$$

where

$$K_1(t) = \frac{a_r(t)}{gG_i}\,\ell$$

$$\bar{x} = x/\ell$$

2. Pressure curvature load. Due to the nature of curvature within real bodies, diametrically opposite bore 'surfaces' possess differing 'areas'. A pressure load acting within this confined chamber will tend to straighten the chamber because the area of the concave 'surface' is greater than its convex counterpart. The expression for this load function (ref 20) is

$$p_2(x,t,y'') = -A_B P_B(t)y''\{H(x_p(t) - x)\} \qquad (24)$$

where

A_B = bore area of tube

$P_B(t)$ = propellant gas pressure

$x_p(t)$ = projectile location

$H(x_p-x)$ = step function

Upon substitution from Eq. (22), the evaluation of the normalized integral yields

$$\frac{1}{G_i}\int_o^{\ell} p_2(x,t,y'')\phi_{ki}\,dx = K_2(t)\int_o^{\bar{x}_p}[\phi_{ki}\sum_{j=1}^{I}\phi''_{kj}q_j + \phi_{ki}y''_s]d\bar{x} \qquad (25)$$

where

$$K_2(t) = - \frac{A_B P_B(t)}{G_i} \ell$$

$$\bar{x}_p = x_p/\ell$$

3. Projectile trajectory load. The accelerating projectile, although of considerably less mass than the tube, can exert a significant transverse force when it is confined to travel along a curved path. Simkins (ref 20) identified this loading and derived the following expression:

$$p_3(x,t,\dot{y}',y'',\ddot{y}) = - \frac{w_p}{g} [\ddot{y} + 2\dot{x}_p(t)\dot{y}' + (\dot{x}_p(t))^2 y'' + g]$$

$$\delta(x_p(t)-x) \qquad (26)$$

where

w_p = projectile weight/unit length

$\delta(x_p(t)-x)$ = Dirac delta function

Upon substitution of Eq. (22) and normalizing with respect to tube length, the integral expression becomes

$$\frac{\ell}{G_i} \int_o^1 p_3(x,t,\dot{y}',y'',\ddot{y}) \phi_{ki} \, \delta(\bar{x}_p(t)-\bar{x}) d\bar{x} =$$

$$K_3 \phi_{ki}(\bar{x}_p)\Big(\sum_{j=1}^{I} \phi_j(\bar{x}_p)\ddot{q}_j + 2\dot{x}_p \sum_{j=1}^{I} \phi_j'(\bar{x}_p)\dot{q}_j +$$

$$(\dot{x}_p)^2 \Big\{ \sum_{j=1}^{I} \phi_j''(\bar{x}_p) q_j + y_s''(\bar{x}_p) \Big\} + g \Big) \qquad (27)$$

where

$$K_3 = \frac{W_p}{G_i g}$$

W_p = projectile weight

4. Projectile eccentricity. Wu (ref 23) has postulated the existence of a couple exerted on the tube when the projectile propelling force does not pass through the projectile's mass center which is expressible as

$$p_4(x,t) = A_B P_B(t)\left(\frac{e_p}{\ell_p}\right)\delta'(x_p-x)\sin(\theta_o+2\pi\tau x_p) \tag{28}$$

where

e_p = radial eccentricity of projectile

ℓ_p = wheelbase of projectile

τ = rifling twist (= 0 for smooth bore)

$$\int_{-\infty}^{\infty} \delta'(x_p-x)dx = 1$$

Upon substitution of Eq. (22) and normalizing, the integral expression becomes

$$\frac{1}{G_i}\int_o^{\ell} p_4(x,t)\phi_{ki}\,dx = -K_4(t)\,\frac{\ell_p}{\ell}\,\phi'_{ki}(\bar{x}_p) \tag{29}$$

where

$$K_4(t) = \frac{A_B P_B(t)}{G_i}\left(\frac{e_p}{\ell_p}\right)\sin(\theta_o+2\pi\tau x_p)\ell$$

5. Projectile rotational load. As the projectile travels along a rifled tube, its mass center rotates causing a centrifugal load on the bore. The vertical component of this reaction is expressible as

$$p_5(x,t) = \frac{w_p e_p}{g\ell}\left[(2\pi\tau\dot{x}_p)^2\delta(x_p-x)\,\sin(\theta_o+2\pi\tau x_p)\right.$$

$$\left. - (2\pi\tau\ddot{x}_p)\cos(\phi_o+2\pi\tau x_p)\right]\delta(x_p-x) \tag{30}$$

where

$\dot{x}_p$ = projectile axial velocity

$\ddot{x}_p$ = projectile axial acceleration

τ = rifling twist in revolutions per inch

Upon substitution and normalization, as above, the integral evaluation becomes

$$\frac{1}{G_i} \int_o^1 p_5(x,t)\phi_{ki}\, d\bar{x} = K_5(t)\phi_{ki}(\bar{x}_p) \tag{31}$$

where

$$K_5(t) = \frac{w_p e_p}{G_i g} [(2\pi\tau\dot{x}_p)^2 \sin(\theta_o+2\pi\tau x_p) - (2\pi\dot{x}_p)\cos(\phi_o+2\pi\tau x_p)]$$

6. Stationary mass reaction. The stationary non-structural masses (breech, bore evacuator, muzzle brake) cause transverse inertial loadings expressible as

$$p_6(x,t,\ddot{y}) = - \frac{w_s}{g} \ddot{y}\delta(x_s-x) \tag{32}$$

where

w_s = weight of stationary mass/length of mass

x_s = axial location of mass

$\bar{x}_s = x_s/\ell$

The integral evaluation is

$$\frac{1}{G_i} \int_o^{\ell} p_6(x,t,\ddot{y})\phi_{ki}\, dx = K_6\phi_{ki}(\bar{x}_s) \sum_{j=1}^{I} \phi_{kj}(\bar{x}_s)\ddot{q}_j \tag{33}$$

where

$$K_6 = - \frac{w_s}{G_i g}$$

W_s = weight of stationary mass

7. Stationary mass eccentricity. Should these masses possess vertical eccentricity with respect to the bore axis, a couple will develop causing a load expressible as

$$p_7(x,t) = - \frac{w_s}{w_R} A_B P_B(t) \left(\frac{e_s}{\ell_s}\right) \delta'(x_s-x) \tag{34}$$

where

W_R = total recoiling weight

e_s = vertical eccentricity from bore axis (+ => above axis)

ℓ_s = wheelbase of eccentric mass

The integral evaluation of this load yields

$$\frac{1}{G_i} \int_o^{\ell} p_7(x,t)\phi_{ki}\, dx = K_7\phi_{ki}'(x_s) \tag{35}$$

where

$$K_7 = - \frac{W_s}{G_i W_R} A_B P_B(t)(e_s)$$

8. Support reactions. The mounting supports may be characterized as non-linear spring elements which react actively with the total displacement of the tube. Initially, the support deflection balances the static loads. As the tube vibrates, the displacements of the tube's support locations change. For a general non-linear support spring, the reactive load may be expressed as

$$p_8(x,t,y) = F_{rn}(y)\delta(x_{rn}-x) \tag{36}$$

where

$F_{rn}(y)$ = dynamic reaction force of n-th support (total reaction - static reaction)

x_{rn} = axial location of n-th support

The integral equation is as follows:

$$\frac{1}{G_i} \int_o^{\ell} p_8(x,t,y)\phi_{ki}\, dx = K_8(y)\phi_{ki}(x_{rn}) \tag{37}$$

where

$$K_8(y) = \frac{F_{rn}(y)}{G_i}$$

9. Bore eccentricity load. Should the gun's bore and outer diameter be non-concentric, each differential segment of the beam contributes an inertia couple about the axis which may be distributed in varying degrees over the full length of the gun. The differential load per unit length may be expressed as follows:

$$p_g(x,t) = -w_k \bar{a}_r(t) e(x_e) \delta'(x_e - x) \tag{38}$$

where

$$\bar{a}_r(t) = \frac{F_B}{W_R} \text{ : normalized acceleration}$$

$$e(x_e) = \text{transverse eccentricity at } x_e$$

Since this is a differential load, its total contribution becomes

$$\frac{1}{G_i} \int_0^{\ell} p_g(x,t)\phi_{ki}dx = -K_g(t) e(\bar{x}_e)\phi_i'(\bar{x}_e)\Delta\bar{x} \tag{39}$$

where

$$K_g(t) = \frac{w_k \bar{a}_r(t) \ell}{G_i}$$

$\Delta\bar{x} = \frac{\Delta x}{\ell}$ = differential length over which the eccentricity is distributed

The total load is the summation of the differential loads. When the formulation is cast in a continuous form, the final value for the load becomes

$$\frac{1}{G_i} \int_0^{\ell} p_g(x,t)\phi_{ki}dx = -K_g(t)\left\{\frac{e(\bar{x})\phi_i(\bar{x})}{\ell}\Big|_{\bar{x}_0}^{\bar{x}_1} - \int_{\bar{x}_0}^{\bar{x}_1} e'(\bar{x})\phi_i(\bar{x})d\bar{x}\right\} \tag{40}$$

Modal Amplitude O.D.E.'s and Numerical Solution Process

The algebraic rearrangement of the loading functions developed in the previous section results in a system of O.D.E.'s in the amplitude vector $q_i(t)$. The general equation is

$$[M]q_i(t) + [C]\dot{q}_i(t) + [K]\dot{q}_i(t) = \sum_{m=1}^{M} f_{mi}(t) \tag{41}$$

where

[M] = inertia matrix of order I

[C] = Coriolis matrix of order I

[K] = stiffness matrix of order I

$f_{mi}(t)$ = i-th mode; m-th load driving force

The three matrices are fully populated unlike the case of a discrete spring, mass, and damper system in which the inertia matrix is diagonal. For the case concerning gun/beam dynamics, the projectile and stationary non-structural masses cause coupling between mode shapes showing up as off-diagonal terms in the inertia matrix. The Coriolis matrix is appropriately named because its only contributing load is due to the moving projectile travelling along a moving path created by the vibrating tube. A Coriolis force component results from this interaction. Modal coupling is a characteristic of this load, therefore, matrix [C] is fully populated. The stiffness matrix [K] contains the natural vibration frequencies (ω_i) along the main diagonal as well as other contributions from recoil inertia, pressure curvature, and projectile trajectory forces. Inclusion of these terms causes the matrix to be fully populated.

The forcing functions on the right side of the equation are all time-dependent in that the ballistic force, recoil inertia, or projectile location and kinematic state are needed for their evaluation. The static slope is required for recoil inertia load evaluation, whereas curvature is needed in the pressure curvature and projectile trajectory loads. Point loads such as those due to projectile location travel along the structure, while those due to the stationary masses are fixed in the spatial coordinate. The support reactions require an evaluation of the total deflection of the tube at their fixed locations with the reaction force being a function of the total displacement.

From a solution standpoint, the problem is quite complex mainly due to the inertia coupling. In order to solve the system of equations using numerical procedures, the matrix [M] must be triangularized by an elimination process (Gauss) with back substitution performed to arrive at a solution to the modal acceleration vector $\ddot{q}_i(t)$. Rearrangement of Eq. (41) and introduction of a discrete time step yields

$$[M]\ddot{q}_i(t_n) = \sum_{m=1}^{M} f_{mi}(t_n) - [C]\dot{q}_i(t_n) - [K]q_i(t_n) \tag{42}$$

where t_n is any integration time. Initially,

$$t_o = 0 \quad \text{and } \dot{q}_i(t_o) = q_i(t_o) = 0 \tag{43}$$

These conditions allow for the startup of the solution process. Equation (42) is solved for $\ddot{q}_i(t_n)$ by back substitution into the triangularized inertia matrix. The resultant acceleration vector is integrated to yield the velocity, and finally the modal displacement vectors.

A predictor-corrector technique, based upon the Adams-Bashforth-Moulton multi-step formulation (ref 24) adapted for systems of equations, was the algorithm chosen for the integration process. A fixed time step with convergence control and limited iteration steps is provided by the user through computer input files. This multi-step method needs four starting values of the function being integrated. These values are generated by using a Taylor series approximation to the solution equation through the four initial time steps. The predictor portion provides an initial solution for the modal velocity and displacement amplitudes by using an integrating algorithm based upon the Adams-Bashforth Four-Step Method. This is an explicit method requiring function evaluations from four preceding time steps. The solution predicted is used in

the corrector portion of the algorithm which is an implicit technique known as the Adams-Moulton Three-Step Method. Iterations on the approximate solution vector continue until convergence is assured based upon a criterion supplied by the user. If the criterion cannot be met in the maximum number of iteration steps, the computer routines report this occurrence allowing for user intervention. Additionally, an error estimate including the number of iterations attempted is available as output for each integration step. This is useful for determining a suitable time step for a given analysis.

RESULTS AND DISCUSSION

At this time, these modelling routines are being debugged and tested against the predictions from standard solutions and other independent analyses. Subsequently, this modelling will be compared with experimental data (both field and laboratory generated) to identify any inherent shortcomings. Parametric studies addressing the projectile's exit vector (see Figure 7, Reference 1) and its sensitivity to perturbations in the design and operational parameters of fielded weapons will follow.

REFERENCES

1. Sneck, H. J. and Gast, R. G., "Normal Modes Analysis of Gun Tube Dynamics," Proceedings of the Fourth U. S. Army Symposium on Gun Dynamics, ARLCB-SP-85009, Vol. I, Benet Weapons Laboratory, Watervliet, NY, 7-9 May 1985, pp. I-22-I-50.

2. Thomson, W. T., Vibration Theory and Applications, Prentice Hall, Englewood Cliffs, NJ, 1965.

3. Timoshenko, S., Young, D. H., and Weaver, W. Jr., Vibration Problems in Engineering, 4th Edition, John Wiley and Sons, New York, 1974.

4. Bozich, W. F., "Transverse Vibration of Nonuniform Free-Free Beams," Masters Thesis, Air Force Institute of Technology, Wright-Patterson Air Force Base, Ohio, 1962.

5. Dolph, C. L., "On the Timoshenko Theory of Transverse Beam Vibrations," Transactions of the ASME, Vol. XII, No. 2, 1953, pp. 175-187.

6. Leibowitz, R. C., and Kennard, E. H., "Shear and Rotatory Inertia Effects on Beam Vibrations," Rep. 1822, David Taylor Model Basin, Washington D.C., July 1964.

7. Kruzlewski, T. T., "Effect of Transverse Shear and Rotatory Inertia on the Natural Frequencies of a Uniform Beam," NACA Tech Note 1909, Washington D.C., 1949.

8. Conte, S. C., Elementary Numerical Analysis, McGraw-Hill, New York, 1965.

9. Wang, H-C., "Generalized Hypergeometric Function Solutions on the Transverse Vibration of a Class of Nonuniform Beams," Journal of Applied Mechanics, September 1967, pp. 702-708.

10. Wang. J. T. S., "Dynamic Analysis of Cantilevered Beams," Paper No. 79-PVP-87, Pressure Vessels and Piping Division of the ASME, June 1979.

11. Lau, J. H., "Vibration Frequencies for a Nonuniform Beam With End Mass," Journal of Sound and Vibration, Vol. 97, No. 3, 1984, pp. 513-521.

12. Goel, R. P., "Transverse Vibrations of Tapered Beams," Journal of Sound and Vibration, Vol. 47, No. 1, 1976, pp. 1-7.

13. Conway, H. D., Becker, E. C. H., and Dubil, J. F., "Vibration Frequencies of Tapered Bars and Circular Plates," Journal of Applied Mechanics, Vol. 31, No. 2, 1964, pp. 329-331.

14. Klein, L., "Transverse Vibrations of Nonuniform Beams," Journal of Sound and Vibration, Vol. 37, No. 4, 1974, pp. 491-505.

15. Mittendorf, S. C., and Greif, R., "Vibrations of Segmented Beams by a Fourier Series Component Mode Method," Journal of Sound and Vibration, Vol. 55, No. 3, 1977, pp. 431-441.

16. Resende, L., and Doyle, W. S., "A Variable Cross-Section 3-D Bear Finite Element for Static and Free Vibration Analysis," Technical Report 806S, Department of Civil Engineering, University of Capetown, South Africa, 1980.

17. Sneck, H. J., Professor, "Two Element Stepped Model," Unpublished notes, 10 pages, Mechanical Engineering Department, Rensselaer Polytechnic Institute, Troy, NY, May 1985.

18. Hibbitt, Karlsson & Sorenson, Inc., "ABAQUS Users Manual Version 4.5(a)," July 1985.

19. Elder, A. J., "Historical Review and Survey of Current Problems in Weapon Dynamics," Proceedings of Dynamics of Precision Weapons, 1977, pp. 1-26.

20. Simkins, T. E., "Transverse Response of Gun Tubes to Curvature-Induced Load Functions," Proceedings of the Second U. S. Army Symposium on Gun Dynamics, ARLCB-SP-78013, Benet Weapons Laboratory, Watervliet, NY, 19-22 September 1978, pp. I-66-I-77.

21. Warken, D., Wolf, K., Heiser, R., Ballmann, J., and Pavel, W. "The Effect of Barrel Curvature and Projectile Unbalance on Excitation of Gun Vibrations," Proceedings of the Third U. S. Army Symposium on Gun Dynamics, ARLCB-SP-82005, Vol. II, Benet Weapons Laboratory, Watervliet, NY, 11-14 May 1982, pp. III-43-III-63.

22. Hall, A. S., Holowenko, A. R., Loughlin, H. G., Theory and Problems of Machine Design, Schaum Publishing Co., New York, 1961, pp. 43-45.

23. Wu, J. J., "On Dynamic Forces in Gun Tube Motions Analysis," Proceedings of the Third U. S. Army Symposium on Gun Dynamics, ARLCB-SP-82005, Vol. II, Benet Weapons Laboratory, Watervliet, NY, 11-14 May 1982, pp. III-85-III-104.

24. Burden, R. L., Faires, J. D., and Reynolds, A. C., Numerical Analysis, Second Edition, Prindle, Weber, and Schmidt, Boston, MA, 1981.

TECHNICAL REPORT INTERNAL DISTRIBUTION LIST

	NO. OF COPIES
CHIEF, DEVELOPMENT ENGINEERING BRANCH	
ATTN: SMCAR-CCB-D	1
-DA	1
-DC	1
-DM	1
-DP	1
-DR	1
-DS (SYSTEMS)	1
CHIEF, ENGINEERING SUPPORT BRANCH	
ATTN: SMCAR-CCB-S	1
-SE	1
CHIEF, RESEARCH BRANCH	
ATTN: SMCAR-CCB-R	2
-R (ELLEN FOGARTY)	1
-RA	1
-RM	1
-RP	1
-RT	1
TECHNICAL LIBRARY	5
ATTN: SMCAR-CCB-TL	
TECHNICAL PUBLICATIONS & EDITING UNIT	2
ATTN: SMCAR-CCB-TL	
DIRECTOR, OPERATIONS DIRECTORATE	1
ATTN: SMCWV-OD	
DIRECTOR, PROCUREMENT DIRECTORATE	1
ATTN: SMCWV-PP	
DIRECTOR, PRODUCT ASSURANCE DIRECTORATE	1
ATTN: SMCWV-QA	

NOTE: PLEASE NOTIFY DIRECTOR, BENET LABORATORIES, ATTN: SMCAR-CCB-TL, OF ANY ADDRESS CHANGES.

TECHNICAL REPORT EXTERNAL DISTRIBUTION LIST

	NO. OF COPIES
ASST SEC OF THE ARMY RESEARCH AND DEVELOPMENT ATTN: DEPT FOR SCI AND TECH THE PENTAGON WASHINGTON, D.C. 20310-0103	1
ADMINISTRATOR DEFENSE TECHNICAL INFO CENTER ATTN: DTIC-FDAC CAMERON STATION ALEXANDRIA, VA 22304-6145	12
COMMANDER US ARMY ARDEC ATTN: SMCAR-AEE	1
SMCAR-AES, BLDG. 321	1
SMCAR-AET-O, BLDG. 351N	1
SMCAR-CC	1
SMCAR-CCP-A	1
SMCAR-FSA	1
SMCAR-FSM-E	1
SMCAR-FSS-D, BLDG. 94	1
SMCAR-MSI (STINFO) PICATINNY ARSENAL, NJ 07806-5000	2
DIRECTOR US ARMY BALLISTIC RESEARCH LABORATORY ATTN: SLCBR-DD-T, BLDG. 305 ABERDEEN PROVING GROUND, MD 21005-5066	1
DIRECTOR US ARMY MATERIEL SYSTEMS ANALYSIS ACTV ATTN: AMXSY-MP ABERDEEN PROVING GROUND, MD 21005-5071	1
COMMANDER HQ, AMCCOM ATTN: AMSMC-IMP-L ROCK ISLAND, IL 61299-6000	1
COMMANDER ROCK ISLAND ARSENAL ATTN: SMCRI-ENM ROCK ISLAND, IL 61299-5000	1
DIRECTOR US ARMY INDUSTRIAL BASE ENGR ACTV ATTN: AMXIB-P ROCK ISLAND, IL 61299-7260	1
COMMANDER US ARMY TANK-AUTMV R&D COMMAND ATTN: AMSTA-DDL (TECH LIB) WARREN, MI 48397-5000	1
COMMANDER US MILITARY ACADEMY ATTN: DEPARTMENT OF MECHANICS WEST POINT, NY 10996-1792	1
US ARMY MISSILE COMMAND REDSTONE SCIENTIFIC INFO CTR ATTN: DOCUMENTS SECT, BLDG. 4484 REDSTONE ARSENAL, AL 35898-5241	2
COMMANDER US ARMY FGN SCIENCE AND TECH CTR ATTN: DRXST-SD 220 7TH STREET, N.E. CHARLOTTESVILLE, VA 22901	1
COMMANDER US ARMY LABCOM MATERIALS TECHNOLOGY LAB ATTN: SLCMT-IML (TECH LIB) WATERTOWN, MA 02172-0001	2

NOTE: PLEASE NOTIFY COMMANDER, ARMAMENT RESEARCH, DEVELOPMENT, AND ENGINEERING CENTER, US ARMY AMCCOM, ATTN: BENET LABORATORIES, SMCAR-CCB-TL, WATERVLIET, NY 12189-4050, OF ANY ADDRESS CHANGES.

TECHNICAL REPORT EXTERNAL DISTRIBUTION LIST (CONT'D)

	NO. OF COPIES
COMMANDER US ARMY LABCOM, ISA ATTN: SLCIS-IM-TL 2800 POWDER MILL ROAD ADELPHI, MD 20783-1145	1
COMMANDER US ARMY RESEARCH OFFICE ATTN: CHIEF, IPO P.O. BOX 12211 RESEARCH TRIANGLE PARK, NC 27709-2211	1
DIRECTOR US NAVAL RESEARCH LAB ATTN: MATERIALS SCI & TECH DIVISION CODE 26-27 (DOC LIB) WASHINGTON, D.C. 20375	1 1
COMMANDER AIR FORCE ARMAMENT LABORATORY ATTN: AFATL/MN EGLIN AFB, FL 32543-5434	1
COMMANDER AIR FORCE ARMAMENT LABORATORY ATTN: AFATL/MNF EGLIN AFB, FL 32542-5000	1
METALS AND CERAMICS INFO CTR BATTELLE COLUMBUS DIVISION 505 KING AVENUE COLUMBUS, OH 43201-2693	1

NOTE: PLEASE NOTIFY COMMANDER, ARMAMENT RESEARCH, DEVELOPMENT, AND ENGINEERING CENTER, US ARMY AMCCOM, ATTN: BENET LABORATORIES, SMCAR-CCB-TL, WATERVLIET, NY 12189-4050, OF ANY ADDRESS CHANGES.

END

DATE

FILMED

MARCH

1988

DTIC